

Nonequilibrium Molecular Dynamics Simulation for Size Effect on Thermal Conductivity of Si Nanostructures

X. J. Liu^{a,c}, Y. W. Yang^b and J. P. Yang^c

^a Nanyang Technological University, Nanyang Avenue, Singapore 639798, liux0014@ntu.edu.sg

^b Nanyang Technological University, Nanyang Avenue, Singapore 639798, cywyang@ntu.edu.sg

^c Data Storage Institute, DSI Building, 5 Engineering Drive 1, Singapore 117608, Yang_Jiaping@dsi.a-star.edu.sg

ABSTRACT

Nonequilibrium molecular dynamics (NEMD) simulation is performed to calculate the thermal conductivity of Si nanostructures. The effectiveness of the Tersoff potential for NEMD simulation of heat transfer is evaluated, and the results display its good performance on heat transfer simulation. Furthermore, the finite size effect related to the system length on the thermal conductivity is studied and the remarkable system size dependence of the thermal conductivity of Si nanostructures is confirmed. Finally, the values of thermal conductivity and mean-free path (MFP) of the infinite bulk Si system are extrapolated based on the simulation results.

Keywords: nanostructure, molecular dynamics simulation, thermal conductivity

1 INTRODUCTION

Thermal characterization of nanostructures is a fundamental issue for the reliability of nano/micro-electromechanical systems (NEMS/MEMS), especially, the thermoelectric effect based energy conversion systems. In these systems, when the size of nanostructures becomes comparable to the inter-atomic distances, their thermal conductivity will be greatly scale-dependent. However, the measurement of thermal conductivity for the nanostructures remains a challenge for the current experimental techniques. The best experimental spatial resolution is still larger than 100 nm [1]. Moreover, interpretation of experiment results remains difficult because typically the influence of experiment environment and individual defects such as impurities, grain boundaries and others, cannot be controlled and analyzed clearly. On the other hand, nonequilibrium molecular dynamics (NEMD) [2, 3] simulation method is an ideal tool for addressing such issues. With theoretical analysis and simulation, NEMD method can provide useful insight on nanoscale heat transfer phenomena.

Since crystalline Si is widely used in NEMS/MEMS, the thermal properties of Si nanostructures are investigated in this paper. For the perfect crystal Si, or the intrinsic and moderately doped Si, the electronic contribution is very small. Thus, the heat transfer due to electrons and radiation

is negligible compared to the phonon heat transfer. Several inter-atomic potentials have been proposed for the NEMD simulation of Si material [4]. However, to the best of the authors' knowledge, only the Stillinger-Weber (SW) potential [5] has been used in the NEMD simulations in the previous studies to calculate the thermal conductivity of Si nanostructures [2, 6]. The SW potentials allows one to accurately simulate the melting temperature and the thermal-expansion coefficient of bulk Si, while the SW potential can not properly handle the characteristic surface structures, low-coordination-number geometries and high-pressure polymorphs [7]. However, the Tersoff potential [8], taking into account the local environment surrounding the bonds, can give more accurate results when applied to both the standard and unconventional geometries. This is a prerequisite for accurate simulation of NEMS/MEMS devices or structures with unconventional geometries. Because, with the decrease of the characteristic size of the nanostructures, the influence of boundary surfaces becomes more and more prominent, which can lead to significant modifications of the vibrational properties of the material compared to its bulk properties. Thus, the Tersoff potential is selected for simulating nanoscale structures and devices. For the thermoelectric effect based energy conversion systems, it is necessary to evaluate the performance of the Tersoff potential in the NEMD simulation of heat transport.

In this paper, the heat transfer properties of perfect crystal Si nanostructures are studied using NEMD with the application of the Tersoff potential. The rest of paper is organized as follows. In the next section, the NEMD simulation methodology and its application to the thermal conductivity are presented. In the third section, the performance of the Tersoff potential on heat transfer simulation is evaluated. The fourth section presents the simulation results and discusses the system size effect on the thermal conductivity of Si nanostructures, followed by the conclusions in the last section.

2 NEMD SIMULATION FOR THERMAL CONDUCTIVITY

Generally, the techniques for simulating heat transfer with the NEMD method numerically mimic a guarded hot plate experiment. The "experiment" system includes a hot thermal reservoir, a cold thermal reservoir, and a sample to

be studied which is placed between the hot and cold thermal reservoirs. The hot and cold thermal reservoirs, consisting of thermostatted sets of atoms, are used to create a temperature gradient in the system, as shown in Figure 1. Upon the creation of these hot and cold regions, it is possible to control the energy given or taken from the thermal reservoir by rescaling the velocity field of the hot and cold regions. With this method, the heat flux can be perfectly controlled to keep constant during the simulation.

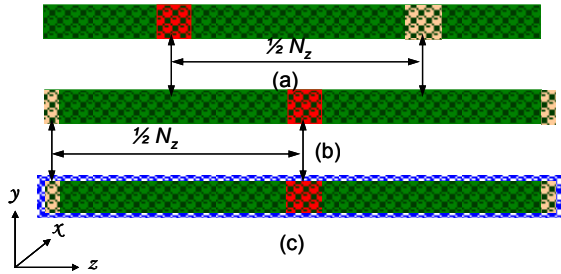


Figure 1 : Geometric configuration of samples: (a) and (b) for periodic boundary condition; (c) for fixed boundary condition. The red represents hot region, the yellow represents cold region and the blue represents fixed region

In this study, the size of the sample is defined by $N_x a_0 \times N_y a_0 \times N_z a_0$ where a_0 ($= 0.5341 \text{ nm}$) is the Si lattice constant, and N_x , N_y , and N_z are the numbers of lattices in the x , y and z directions respectively, as shown in Figure 1. The hot and cold thermal reservoirs consist of sets of atoms forming a slice parallel to the xy plane so that heat transfer is uni-dimensional in the z direction. The size of the simulation system and the locations of the hot and cold thermal reservoirs depend on the boundary conditions, as shown Figure 1(a), (b) and (c). For the periodic boundary conditions (PBC), the system has the same size as the sample. For the fixed boundary conditions (FBC), the size of the system is larger than the sample size by at least the cut-off distance of the Tersoff potential, 0.30 nm .

The thermal conductivity relates the heat flux to the temperature gradient via the Fourier's law as follows

$$k(T) = -\frac{J_z}{\nabla T_z} \quad (1)$$

where k is the thermal conductivity, J_z ($= \Delta \varepsilon / 2At$) is the heat flux defined as the amount of heat energy ($\Delta \varepsilon$) transferred per unit time (t) through unit area (A) perpendicular to the direction of the heat flux, and $\nabla T_z = \partial T / \partial z$ is the temperature gradient in the z direction, which is calculated using NEMD.

To calculate the temperature gradient, the simulation system is divided into j slices along the z direction. The temperatures of the slices are calculated in each iteration. After the system reaches at the equilibrium status, a heat flux is imposed on the system along the z direction. A small amount of kinetic energy, $\Delta \varepsilon$, is added in the hot thermal reservoir. Simultaneously, the same amount of energy is

removed from the cold thermal reservoir. The hot and cold thermal reservoirs can be located anywhere in the sample, but the distance between them should be a half length of the sample because of the PBC.

3 MD SIMULATION OF HEAT TRANSFER USING THE TERSOFF POTENTIAL

As shown in Figure 1(a), a parallelepiped system with a three-dimensional PBC is selected in this study for heat transfer simulation. The size of the simulation system is $2a_0 \times 2a_0 \times 144a_0$. The equilibrium temperature is set at 500K. The energy increment is $\Delta \varepsilon = 4.3 \times 10^{-4} \text{ eV}$ [9], and the time step is $\Delta t = 0.57 \text{ fs}$. The system is divided into 144 slices along the z direction. The size of each slice is $2a_0 \times 2a_0 \times 1a_0$, thus there are 32 atoms in each slice, which satisfies the recommendation of Mait et al. [10].

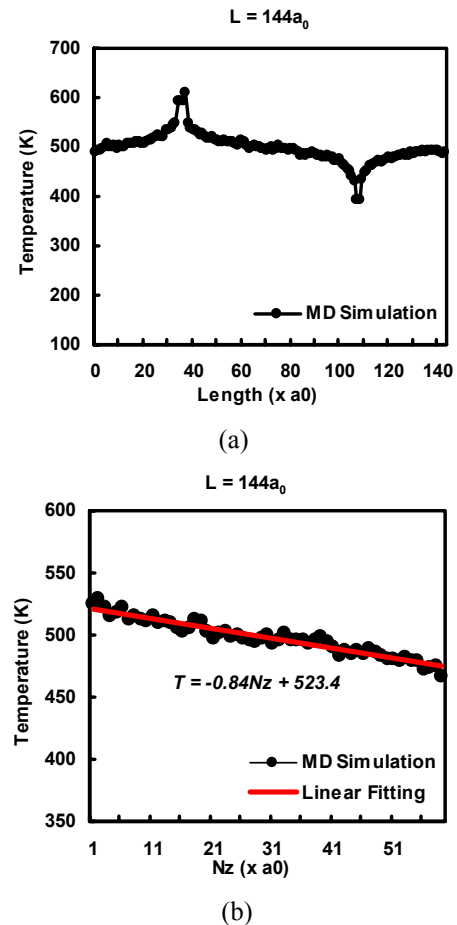


Figure 2 (a) Temperature profile for $2a_0 \times 2a_0 \times 144a_0$ at 500K; (b) Least-square linear fitting of temperature profile in the region between the hot and cold reservoirs.

Under these conditions, the NEMD simulation shows that a steady status is attained after about 200,000 time steps. Subsequently, the simulation continues for another

2,000,000 time steps (~ 1.08 ns) to achieve a good accuracy in the temperature gradient between the hot and cold reservoirs.

The temperature profile of the system is shown in Figure 2(a) in the direction of heat transfer. As expected, near the hot/cold reservoirs, strong nonlinear temperature profiles are observed, which can be attributed to the strong phonon scattering that occurs at the interfaces with the hot and cold thermal reservoirs [9, 11, 12]. In order to reduce the effect of high scattering at the thermal reservoirs and focus on the temperature distribution between the reservoirs, several slices close to the thermal reservoirs are excluded in the temperature profile, as plotted in Figure 2(b). The calculated temperature is denoted by the bold dots and the least-square linear fitting is given for the intermediate region between the hot and cold reservoirs. From the linear fitting, the temperature gradient can be readily obtained as $\partial T/\partial z = 0.84$ K/ a_0 . The heat flux and the thermal conductivity can be calculated from Eq. (1) as $J_z = \Delta\epsilon/(2N_x a_0 \cdot N_y a_0 \cdot \Delta t) = 51.27 \times 10^9$ Jm⁻²s⁻¹ and $k = 33.34$ WmK⁻¹, respectively. The value of k is very close to that (~ 34 WmK⁻¹) predicted by Schelling [11] using SW potential. Thus, the suitability of the Tersoff potential for NEMD simulation of heat transfer can be validated.

4 FINITE-SIZE EFFECT ON THERMAL CONDUCTIVITY

Finite-size effect arises when the length of the simulation sample is comparable to the phonon mean-free path (MFP) [12]. For a sample with length smaller than the MFP in an infinite system, the thermal conductivity will be limited by the system size. This regime is known as the Casimir limit.

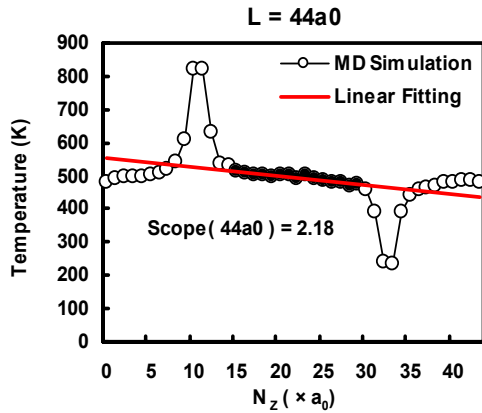


Figure 3 Temperature profile for $2a_0 \times 2a_0 \times 44a_0$ at 500K. Red line represents the least-square linear fitting of temperature profile in the region between the hot and cold reservoirs with the slope of 2.18 K/ a_0 .

In this work, NEMD simulations for various sample lengths, l_z , have been performed. The size of system is fixed at $2a_0$ in both the x and y directions, but varies from $44a_0$ to $144a_0$ in the z direction. For a unit cell, there are eight Si

atoms and for the largest system ($2a_0 \times 2a_0 \times 144a_0$), there are 4608 atoms. Figure 3 shows the temperature profile for the sample with $44a_0$ at temperature 500K, and the least-square linear fitting of temperature profile in the region between the hot and cold reservoirs. The temperature profiles for the samples with other lengths are similar to Figure 3, not shown, while the least-squares linear fitting for these samples are plotted in Figure 4.

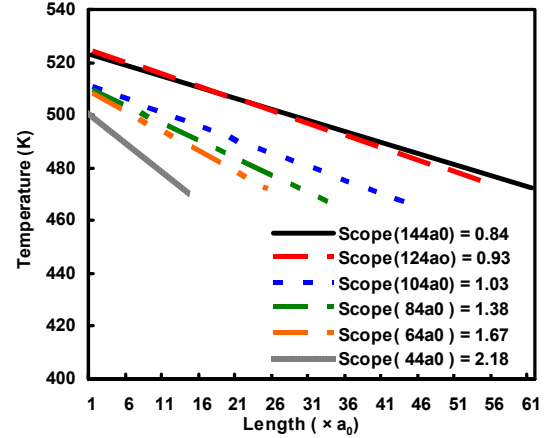


Figure 4 Least-square linear fitting of temperature profiles in the region between the hot and cold reservoirs of the systems with various lengths ($44a_0$, $64a_0$, $84a_0$, $104a_0$, $124a_0$ and $144a_0$).

As shown in Figure 4, it is noted that the heat transfer increases with the increase of system size. According to these results, the values of k for different system lengths are shown in Table 1.

L_z ($\times a_0$)	$\partial T/\partial z$ ($\times 10^9$ k/m)	k (W/mk)	k' (W/mk)
44	4.01	12.80	8.07 [13]
64	3.07	16.72	-
84	2.54	20.15	-
104	1.90	26.95	-
124	1.72	29.81	-
144	1.54	33.34	34 [11]

Table 1 Comparison of k for various system lengths l_z

It is found that the thermal conductivity exhibits a strong dependence on the system size. Based on the phonon gas kinetic theory, $k = \frac{1}{3} c v l_{eff}$, the mechanism of this dependence can be expressed by the following equation approximately [11]:

$$\frac{1}{k} = \frac{a_0^3}{k_B v} \left(\frac{1}{4l_\infty} + \frac{1}{l_z} \right) \quad (2)$$

where $c = \frac{3}{2} k_B n$ is the specific heat of phonons, $l_{eff} = (1/l_\infty + 4/l_z)^{-1}$ is the effective MFP, $n = 8/a_0^3$ is the

number density of atoms in the system, v (≈ 6500 m/s) is the group velocity of an acoustic branch, and l_∞ is the MFP for an infinite system. By setting $1/l_z = 0$ in Eq. (2), the thermal conductivity of an infinite system can be obtained. Eq. (2) also shows the linearity between $1/k$ and $1/l_z$.

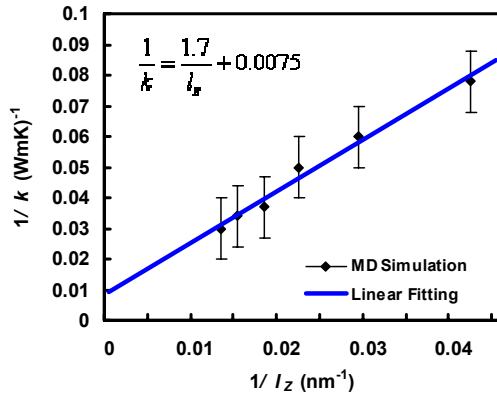


Figure 5 System size dependence of $1/k$ on $1/l_z$ at 500K.

The calculated thermal conductivities in Table 1 and the least-square linear fitting of $1/k$ on $1/l_z$ are illustrated in Figure 5. The figure shows that $1/k$ and $1/l_z$ have strong linear relationship which is in accordant with Eq. (2). The slope is $1.7 \times 10^{-9} \text{ m}^2\text{K/W}$ obtained using the Tersoff potential. This value is comparable to the results obtained using the SW potential by Broughton [14] ($\sim 1.8 \times 10^{-9} \text{ m}^2\text{K/W}$) and Schelling [11] ($\sim 2.0 \times 10^{-9} \text{ m}^2\text{K/W}$).

Using the above linear fitting, we can also estimate the thermal conductivity of bulk Si $k = 133 \text{ W/mK}$ by setting the limit $1/l_z = 0$ at 500K. This result again is comparable to 120 W/mK predicted by the experimental data for the isotropically enriched Si at 500K in [15]. The discrepancy between the simulated and testing results may be attributed to the fact that for the natural Si, defect scattering significantly reduces the thermal conductivity k , but no defect scattering has been considered in the simulation. Thus the simulated k is about 10% higher than the experimental value. Based on the extrapolated value of k , the MFP l_∞ for the bulk Si can also be estimated at about 62 nm , which is reasonable according to the reported results [10, 16].

5 CONCLUSION

This paper proposed the use of the Tersoff potential for NEMD simulation to determine the thermal conductivity of nanoscale structures and devices. The simulated thermal conductivity of Si is well consistent with the result using the SW potential based simulation and by experiment. The suitability of the Tersoff potential for heat transfer simulation was thus validated. Furthermore, the finite-size effect on the thermal conductivity was studied. The remarkable system size dependence of the thermal conductivity of Si nanostructures was confirmed, which qualitatively may be caused by the factors that the effective

phonon MFP is greatly reduced when the size of simulation system is smaller than that of bulk Si, and the number of phonons which contribute to the heat transfer or thermal capacity is limited when the size of simulation system is finite. The extrapolated results of thermal conductivity and MFP for the infinite bulk Si system are also comparable to the reported simulated and experimental results.

Due to the PBC used in the present simulation system, phonons are free to travel across the system boundaries perpendicular to the heat flux direction without scattering in any obvious way. It is expected that the thermal conductivity will not depend as sensitively on the dimensions perpendicular to the heat flux as on the length. The effects of different transverse areas and different boundary conditions (i.e. periodic, fixed, free boundary surfaces) on the thermal conductivity are under investigation.

REFERENCES

- [1] Deyu Li, Yiying Wu, Philip Kim, Li Shi, Peidong Yang and Arun Majumdar, Applied Physics Letters, 83, 2934, 2003
- [2] Aron Cummings, Mohamed Osman, Deepak Srivastava, and Madhu Menon, Physical Review B, 70, 115405, 2004
- [3] P. Chantrenne and J. L. Barrat, Journal of Heat Transfer, 126, 577, 2004
- [4] Stephen J. Cook and Paulette Clancy, Physical Review B, 47, 7686, 1993
- [5] Frank H. Stillinger and Thomas A. Weber, Physical Review B, 31, 5262, 1985
- [6] P. Chantrenne, J. L. Barrat, X. Blasé and J. D. Gale, Journal of Applied Physics, 97, 104318, 2005
- [7] Brian W. Dodson, Physical Review B, 337361, 1986
- [8] J. Tersoff, Physical Review Letters, 56, 632, 1986
- [9] Philippe Jund and Remi Jullien, Physical Review B, 59, 13707, 1999
- [10] A. Maiti, G. D. Mahan and S. T. Pantelides, Solid State Communications, 102, 517, 1997
- [11] Patrick K. Schelling, Simon R. Phillpot, and Pawel Keblinski, Physical Review B, 65, 144306, 2002
- [12] C. Oligschleger and J. C. Schon, Physical Review B, 59, 4125, 1999
- [13] Qiheng Tang, Molecular Physics, 102, 1959 (2004)
- [14] J. Q. Broughton and X. P. Li, Physical Review B, 35, 9120, 1987
- [15] W. S. Capinski, H. J. Maris, E. Bauser, I. Sillier, M. Asen-Palmer, T. Ruf, M. Cardona, and E. Gmelin, Applied Physics Letters, 71, 2109, 1997
- [16] A. D. McConnel and K. E. Goodson, Annual Review of Heat Transfer, 14, 129, 2005